

LASER SPECTROSCOPY

PACS numbers: 42.62.Fi; 34.35.+a; 32.10.Fn
DOI: 10.1070/QE2013v043n09ABEH014772

Laser spectroscopy of sub-micrometre- and micrometre-thick caesium-vapour layers*

S. Cartaleva, A. Krasteva, L. Moi, A. Sargsyan, D. Sarkisyan, D. Slavov, P. Todorov, K. Vaseva

Abstract. **We present high resolution laser spectroscopy of Cs vapours confined in a unique optical cell of sub-micrometric and micrometric thickness, where a strong spatial anisotropy is present for the time of interaction between the atoms and laser radiation. Similarly to the spectra of selective specular reflection, the Doppler-free spectra of absorption and fluorescence are observed, not revealing cross-over resonances that will be useful for frequency stabilisation, provided the cell is cheap and compact. A new resonance in the fluorescence of closed transition is studied, demonstrating its high sensitivity to elastic atom–atom and atom–dielectric surface collisions. The theoretical modelling performed is in agreement with the experimental observations.**

Keywords: *high-resolution laser spectroscopy, nanometric atomic vapour layers, transient effect in a nanometre-thin cell.*

1. Introduction

High resolution laser spectroscopy of alkali vapour contained in conventional thermal optical cells with centimetre dimensions is widely used in various applications such as wavelength references, atomic clocks, precise optical magnetometers, slow and stored light, photonic sensors based on coherent population trapping (CPT) and electromagnetically induced transparency (EIT) resonances, etc. For these applications, the reduction of optical cell dimensions is of significant importance.

Our paper is devoted to high resolution laser spectroscopy of alkali vapour confined in a unique nanometre-thick optical cell [1], further on called an extremely thin cell (ETC). An interesting peculiarity is that the dimensions of such a cell differ significantly. The distance L between the high-optical-quality cell windows varies from 30 nm to 1–6 μm. At the same time, the window diameter is about 2 cm. Therefore, strong spatial anisotropy is present for the time of interaction between alkali atoms confined in the ETC and laser radiation, which leads to a strong reduction in the Doppler effect influence on spectral lines. Mainly two groups of atoms can be distinguished: 'slow' and 'fast'. Slow atoms involve those flying predominantly in the direction orthogonal to the laser beam (typically of one-millimetre diameter) and reach the steady state in the interaction with the laser light. Fast atoms have a significant velocity projection on the laser beam propagation direction; as a result, the time of atomic flight between the ETC windows is shorter than the lifetime of the excited state of the atom. This anisotropy leads to a significant difference between the observed fluorescence and transmission (absorption) spectra and to the appearance of sub-Doppler-width (SDW) resonances centred at optical transitions.

It was found that at a low pump intensity (unsaturated regime), the linewidth of the absorption of the hyperfine transition exhibits an oscillating behaviour and has a minimum value when $L = (2n + 1)\lambda/2$, and a maximum value when $L = n\lambda$ (n is an integer, λ is the wavelength of the irradiating light). This was determined as the manifestation of the so called collapse and revival of a Dicke-type coherent narrowing effect [2]. Also the magnitude of the absorption shows an oscillating behaviour. The effect of optical transition narrowing has been observed for L up to $\frac{7}{2}\lambda$. Note that in contrast to the transmission spectra, when L increases, the linewidth of the fluorescence spectra increases monotonically, while remaining below the Doppler broadening even when the thickness of the vapour column increases up to a few micrometres. The fluorescence magnitude smoothly increases with L as well [3–6].

To briefly discuss the coherent Dicke narrowing, it is worthy of note that the effect of atom–wall collisions, strongly disturbing the internal atomic state, leads to a narrower spectral line than that obtained in the absence of such collisions. In case of a dilute atomic vapour, an atom continues to radiate until it hits the cell window surface. In the absence of such a collision, the atomic motion would mix atoms oscillating with different phases, resulting in a destructive interference between contributions from individual atoms. If $L \leqslant \lambda/2$ and the atomic radiation times are longer than their time of flight between the two windows, the slow atoms will have an advantage because they are excited for a longer time and radiate for a longer period. Because of the long uninterrupted radiation, slow atoms contribute to the absorption at the centre of atomic transition, strongly enhancing it, which results in an atomic transition narrowing [2, 7].

*Presented at the 19th International Conference on Advanced laser technologies (ALT'11), Bulgaria, Golden Sands, September 2011.

S. Cartaleva, A. Krasteva, D. Slavov, P. Todorov, K. Vaseva Institute of Electronics, Bulgarian Academy of Sciences, boul. Tzarigradsko shosse 72, 1784 Sofia, Bulgaria; e-mail: stefka-c@ie.bas.bg;
L. Moi CNISM and Physics Department, University of Siena, via Roma 56, 53100 Siena, Italy;
A. Sargsyan, D. Sarkisyan Institute for Physical Research, National Academy of Sciences of Armenia, Ashtarak-0203, Armenia

Received 9 November 2011; revision received 12 May 2012
Kvantovaya Elektronika **43** (9) 875–884 (2013)
Submitted in English

The main peculiarities of fluorescence and absorption spectra of Cs atoms confined in ETCs will be presented and analysed using the theoretical model developed in Ref. [8]. In such a strongly confined atomic ensemble a series of SDW resonances occurs [9], which are subject to intensive study, motivated by the possible applications for development of wavelength references as well as for investigation of atom–atom and atom–cell window collisions. The results presented will be related to SDW resonance preparation in ETCs with a thickness ranging from $L = \lambda$ to $L = 6\lambda$, where $\lambda = 852$ nm is the wavelength of the laser light that is resonant with the D_2 line of caesium.

The study of ETC properties will make possible further miniaturisation of optical cells used in photonic sensors based on CPT/EIT without a buffer gas. The strong reduction in the cell dimensions would require utilisation of a very high pressure buffer gas, decreasing the efficiency of atomic excitation by the laser light.

2. Experimental

In this section, after a brief description of the optical transitions in question and the experimental setup employed, we present the experimental results on fluorescence and transmission spectra obtained in the ETC containing Cs vapour.

The diagram of ^{133}Cs energy levels with the hyperfine transitions on the D_2 line is shown in Fig. 1. The D_2 line consists of two sets of hyperfine transitions, forming two absorption (fluorescence) lines: (i) the $F_g = 3$ set, involving three transitions from the $F_g = 3$ ground level to the respective $F_e = 2$, 3 and 4 excited levels and (ii) the set of $F_g = 4$ transitions. In the widely used optical cells with centimetre dimensions (further on called conventional), the hyperfine transitions starting from single ground level completely overlap due to the Doppler broadening (~400 MHz). Thus, the two types of transitions ($F_g \to F_e \leqslant F_g$ or $F_g \to F_e > F_g$) involved in the absorption line cannot be resolved (see Ref. [10]). However, they have different properties. The first type ($F_g \to F_e \leqslant F_g$ transition) always suffers population loss from the ground level irradiated by the light due to hyperfine or Zeeman optical pumping caused by the excited state fluorescent decay, while the second type ($F_g \to F_e > F_g$ transition) is considered completely closed in the absence of hyperfine optical pumping [11]. The situation is different in the ETC. Here, as shown in previous works, the hyperfine transitions within a single absorption (fluorescence) line can be resolved [8, 11]. Hence one can investigate separately the two types of hyperfine transitions, which are involved in the absorption (fluorescence) line.

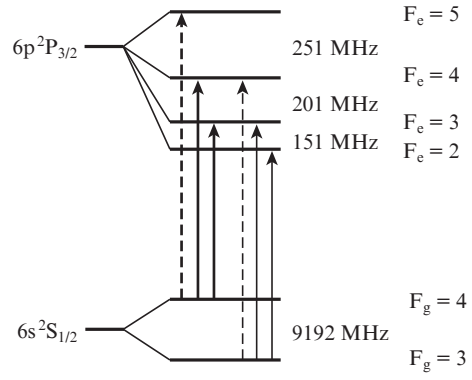

Figure 1. Energy-level diagram for D_2 line of ^{133}Cs. $F_g \to F_e \leqslant F_g$ transitions (solid line) differ from $F_g \to F_e > F_g$ transitions (dashed line).

The scheme of the experimental setup is presented in Fig. 2. A single-frequency distributed feedback diode laser (DFBL) with a low-noise power supply and about 2 MHz linewidth was used. The DFBL emission wavelength was precisely tuned by varying its current. The laser light was linearly polarised and its frequency was scanned over the set of $F_g = 4$ or $F_g = 3$ transitions. The laser beam was directed to the ETC containing Cs vapour, orthogonally to the surface of its windows. Two ETCs were used in the experiment. The first ETC design is similar to that described in [9], but in our case the thickness of the vapour layer may vary in a range of 100–2800 nm. For this cell, the laser beam diameter was 0.9–1 mm, which provides less than $\lambda/4$ cell thickness variation within the laser beam cross section. The overall thickness variation range is realised by a preceding deposition of the Al_2O_3 layer of controlled thickness onto the surface of one of the ETC windows in its lower part. The wedge-shaped (along the vertical direction) thickness of the ETC was measured by applying the interference technique. The ETC was placed in an oven with three ports, two of which were used for the laser-beam transmission, and the third port – for the fluorescence collection in the direction orthogonal to the laser beam. Thus, we could detect the fluorescence and the transmission spectra simultaneously.

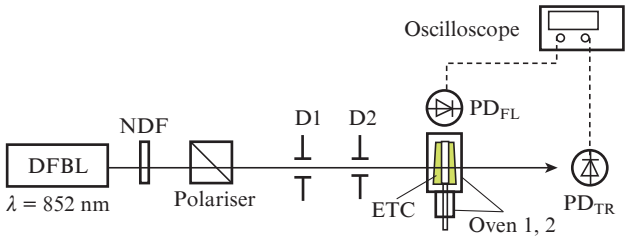

Figure 2. Experimental setup: (NDF) neutral density filter; (D1, D2) diaphragms; (PD_{FL}, PD_{TR}) fluorescence and transmission detectors.

The second cell was a so called multipurpose cell having three sectors of different thickness. In this work we used only one section with $L = 6\lambda$, where the region of constant thickness L is about 6 mm. Here the laser beam diameter was 3 mm. Both ETCs were sealed-off optical cells with no buffer gas added, and were filled by Cs vapour from a small Cs container situated in a side arm connected to the cell. In some of the experiments, the cell of thickness $L = 6\lambda$ was placed in the magnetic shield protecting the cell against the Earth and laboratory magnetic fields. No significant difference in the measured spectra was observed when applying such shielding.

The Cs vapour absorption (transmission) and fluorescence spectra were measured at different L, atomic source temperatures and light intensities.

2.1. Transmission and fluorescence for the set of $F_g = 3$ transitions of Cs vapour confined in ETCs

To study the saturation of open transitions, we will first present the transmission (absorption) spectra of the set of $6S_{1/2}$

($F_g = 3$) → $6P_{3/2}$ ($F_e = 2, 3, 4$) transitions (Fig. 3), which contains only open transitions, i.e. atomic transitions suffering the population loss to energy level non-interacting with the laser light. The population loss is caused by hyperfine and/or Zeeman optical pumping processes, based on the spontaneous decay from the excited levels. Note that the $F_g = 3 \rightarrow F_e = 2$ transition is closed in term of hyperfine optical pumping but it suffers population loss from the ground Zeeman sub-levels excited by the light due to optical pumping to Zeeman sub-levels non-interacting with the laser light. Hence, this transition is defind as an open transition.

Unlike Refs [8, 9], a new developed laser system was used with DFB laser source and extremely low noise current controller. This system allowed us to achieve strong improvement of spectral resolution and signal-to-noise ratio during the registration of atomic spectra. From Fig. 3 it can be seen that within the $F_g = 3$ absorption line three very narrow and well-pronounced enhanced transmission/absorption SDW resonances are observed, centred at the hyperfine optical transitions. The SDW structure (with typical FWHM of 15 MHz, which is more than 25 times less than the Doppler width of the transitions) can be registered at a lower light intensity than in Ref. [9]. This makes it possible to observe simultaneously enhanced absorption narrow features at $L = 1.5\lambda$ due to the Dicke effect [3, 4] (first Dicke revival) and enhanced transmission peaks at $L = \lambda$, 2λ and 3λ. Note that although at $L = 2.5\lambda$ the second Dicke revival is not observed, the Dicke effect contribution is well expressed as some broadening and amplitude reduction in the SDW resonances.

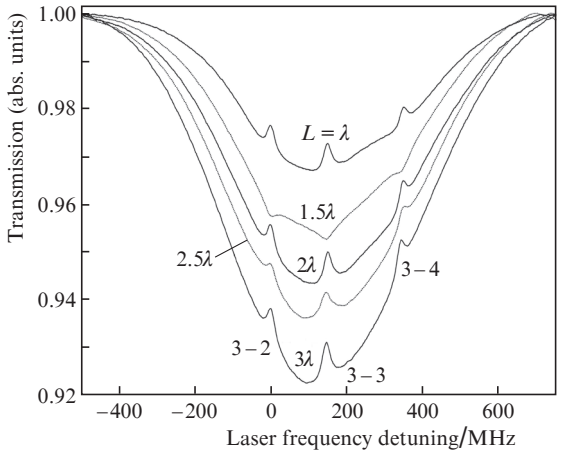

Figure 3. Transmission spectra on the $F_g = 3$ line at different L. The atomic source temperature is $T = 98\,^{\circ}C$, atomic density is $\sim 1.2 \times 10^{13}$ atom cm^{-3} and light intensity is $W = 6$ mW cm^{-2}.

Consequently, based on the transmission spectrum of the few-micron-thick ETC, a frequency reference can be developed with very good sub-Doppler-width precision. It should be stressed that unlike the case of saturated absorption (SA) technique [12], based on spectroscopy of two counterpropagating beams in conventional cells, in the ETC approach the transmission spectrum is measured by a simple and robust single-beam optical system. Such a system is promising for building practical devices, provided the ETC is cheap and compact.

As reported in Ref. [8] for ETCs with $L = \lambda$, with increasing light intensity tiny SDW features of reduced fluorescence have been obtained in the fluorescence profiles of open transitions only. Figure 4 shows the fluorescence spectra at $L = \lambda$ and 3λ. In the case of a cell with $L = \lambda$, the SDW fluorescence dips (which are marked by asterisks) are of extremely small amplitude (slightly higher than the experimental noise). Their examination was performed by phase sensitive registration [8]. Note that in the fluorescence spectra, the Doppler profiles of the hyperfine transitions are well resolved (particularly at $L = \lambda$), which is opposite to the Doppler profile behaviour in the transmission spectra (Fig. 3). This result is in good agreement with previous works [1, 8, 9] as well as with our calculations (see Section 3).

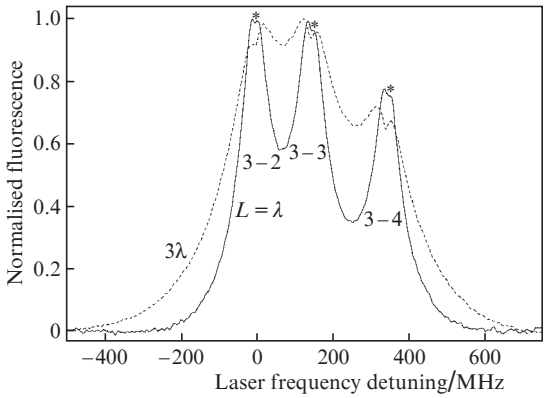

Figure 4. Fluorescence spectra of the set of $F_g = 3$ transitions at $L = \lambda$ and 3λ, $W = 6$ mW cm^{-2} and atomic density $\sim 1.2 \times 10^{13}$ atom cm^{-3}.

Later on, we showed [9] that with increasing ETC thickness up to $L = 3\lambda$ the reduced fluorescence dips increase their amplitudes. However, in [9] the spectral width of the emission of the diode laser system used was about 15 MHz, which was a reason for a significant broadening of the dips observed in the fluorescence and strong reduction in their amplitude. Here, we present the fluorescence profile study up to $L = 6\lambda$ with strongly improved spectral resolution.

Following the theoretical simulations presented in Section 3, which allowed us to predict large enhancement of the fluorescence dip contrast with the increasing cell thickness, a systematic experimental study is performed for the ETC with $L = 6\lambda$. Figure 5 shows the fluorescence spectrum for the $F_g = 3 \rightarrow F_e = 2, 3, 4$ transitions observed in the ETC with $L = 6\lambda$. It can be seen that increasing the cell thickness from λ to 6λ, narrow and very good contrast dips in the fluorescence are obtained. In the ETC with $L = 6\lambda$, the width $\Delta\nu$ of the reduced fluorescence dip is quite low: $\Delta\nu = 12$ MHz (Fig. 5). In addition, it should be pointed out that for the cell with $L = 6\lambda$, the overlapping of hyperfine transition Doppler profiles is much stronger than for the cell with $L = \lambda$. Hence, in the former case atoms belonging to a broader atomic velocity class participate in the process of fluorescence, which is provided by the enhanced time of flight of atoms between the ETC windows.

A significant increase in the amplitude of the reduced fluorescence SDW dips can be achieved by increasing slightly the light intensity (Fig. 5). One can see that the resonance contrast can be improved by more than an order of magnitude when using the ETC with $L = 6\lambda$ at an order of magnitude less light intensity than in case of the cell with $L = \lambda$. Hence, our experiments confirm the theoretical prediction that a small (few micrometres) enlargement of the ETC thickness will pro-

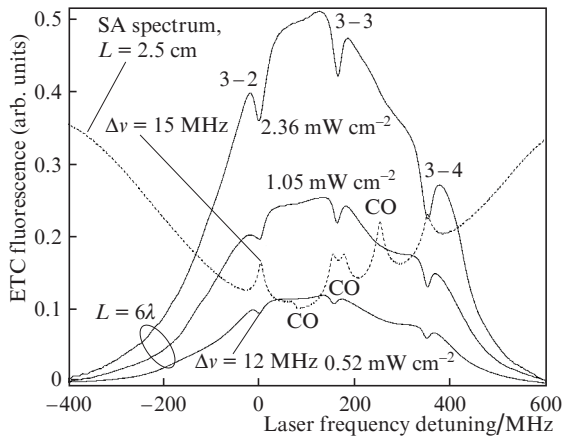

Figure 5. Fluorescence spectra of the set of $F_g = 3$ transitions for a cell with $L = 6\lambda$ and at different intensities; $T = 68\,^{\circ}C$, the atomic density is $\sim 1.5 \times 10^{12}$ atom cm^{-3}. For comparison the SA spectrum of a conventional cell is shown.

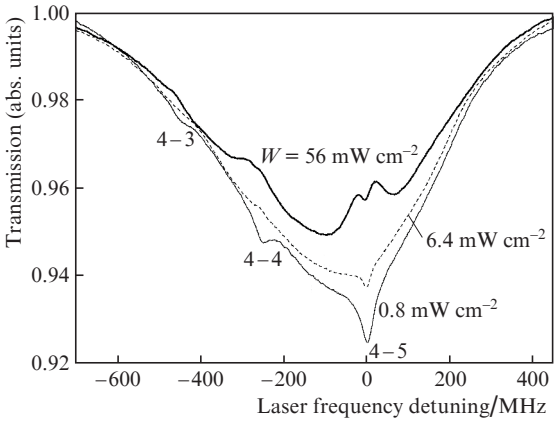

Figure 6. Transmission spectra of the set of $F_g = 4$ transitions at different intensities and atomic density $\sim 1.2 \times 10^{13}$ atom cm^{-3}; $T = 98\,^{\circ}C$; $L = 1.5\lambda$. Under condition of the first revival of the Dicke effect, the difference in the saturation behaviour of open and completely closed atomic transitions is clearly seen.

vide significant improvement in the signal of the reduced fluorescence dip while keeping its spectral width small. A result worthy of note is that the frequency reference spectrum shown in Fig. 5 consists of very well resolved components, the positions of the components coincide with the frequencies of the three hyperfine transitions, and the spectrum is measured by simple means of single beam spectroscopy. The enhancement of the ETC thickness up to $L = 6\lambda$ not only provides the possibility for strong reduction in the light intensity but also allows working at a lower atomic source temperature, which is of significant importance for operating practical frequency reference devices.

For comparison with the ETC spectra, Fig. 5 shows a saturated absorption spectrum measured by the conventional two-counterpropagating-beam technique [8]. It is clearly seen that the saturated absorption spectrum observed in a cm-sized cell is more complicated than the three-narrow-resonance spectra in the ETC transmission and fluorescence. Note that even at an enhanced thickness of $L = 6\lambda$, the anisotropy in the time of atom-light interaction still suppress the formation of crossover (CO) resonances in the ETC.

2.2. Transmission and fluorescence for the set of $F_g = 4$ transitions of Cs vapour confined in ETCs

In this section we present a significantly improved spectral resolution (compared to that of Ref. [9]) investigation of the difference between the saturation of open and closed transitions under conditions of strongest Dicke revival, namely at $L = 1.5\lambda$. The experimentally obtained spectra are shown in Fig. 6. For the light intensity of 0.8 mW cm^{-2}, one can distinguish all three hyperfine transitions due to the narrow Dicke peak in absorption, centred at each atomic transition. The SDW enhanced absorption feature originates from the coherent atom–light interaction in transient regime, and it is associated with the Dicke narrowing [2–5].

With increasing light intensity, a reduction in the amplitude of the narrow Dicke features occurs for both open $F_g = 4 \rightarrow F_e = 3, 4$ transitions. Further on, saturation dips of reduced absorption at atomic transition centres start to appear. The two dips grow in amplitude and their width increases with light intensity.

In case of the completely closed $F_g = 4 \rightarrow F_e = 5$ transition, however, the saturation with the light intensity is more complicated. The reduced absorption dip is not the only SDW feature that is recognisable in the absorption spectrum with the light intensity increasing. In addition, at the $F_g = 4 \rightarrow F_e = 5$ transition, there is a well pronounced Dicke absorption peak (even at the highest intensity), which is superimposed on the saturation dip. By increasing the light intensity, one can see that the Dicke signal does not change notably its amplitude although it falls in the saturation dip, which grows fast in amplitude with increasing light intensity. Note also that the width of the Dicke enhanced absorption resonance does not change significantly with the light intensity. It has to be mentioned that the $F_g = 4 \rightarrow F_e = 5$ transition is defined as completely closed because neither hyperfine nor Zeeman optical pumping occurs at this transition, i.e. there is no ground Zeeman sublevels non-interacting with the laser light.

In general, it can be concluded that the saturation behaviour in the absorption of open and closed transitions is very different in the presence of the Dicke coherent narrowing of optical transition. The Dicke signal at the closed transition is quite robust against the saturation of the optical transition. The reason for such a difference could be found in the transient effects of atom–light interaction, intrinsic to the nature of the ETC, combined with the optical pumping (in a three-level system) or with the saturation effects in a two-level system. It is well known [4–6] that the Dicke narrowing results in the appearance of a narrow Dicke signal over the Doppler broadened pedestal, where the Dicke signal originates from the transient effects. The significant contribution to the narrow Dicke signal comes from the slow atoms. However, namely the slow atoms suffer the highest loss due to the optical pumping to the ground-state level non-interacting with the light, which occurs in case of the open transitions. Hence, at the open transitions, the Dicke signal is absent at higher light intensities.

The investigation of the absorption and fluorescence of the confined media in question started in the weak-intensity regime [3], and the work was concentrated mainly on the investigation of the absorption spectra, considering that the fluorescence profiles exhibit only monotonic broadening with the cell thickness [4]. For a low light intensity, our investiga-

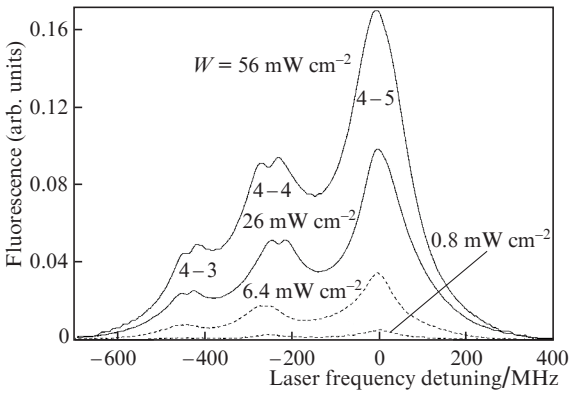

Figure 7. Fluorescence spectrum, observed in the ETC of thickness $L = 1.5\lambda$ for the set of $F_g = 4$ transitions at $T = 98\,^{\circ}C$ and atomic density $\sim 1.2 \times 10^{13}$ atom cm^{-3}. No dip is observed in the fluorescence profile of the $F_g = 4 \rightarrow F_e = 5$ transition.

tions confirm the monotonic broadening of the fluorescence profiles with increasing ETC thickness. However, as discussed at the end of Section 2.1, the saturation dip of reduced fluorescence starts to appear in the narrow fluorescence profiles of open transitions when irradiating the ETC with $L = \lambda$ by a higher intensity laser light. The dip amplitude enhances with increasing cell thickness and light intensity (Figs 4, 5). Previous studies [8] have shown no saturation dip in the fluorescence of the closed $F_g = 4 \rightarrow F_e = 5$ transition at $L = \lambda$.

Here we present experimental results, obtained by means of the narrow band laser system. The significant difference between the saturation behaviour of the fluorescence profiles of the open and closed transitions is illustrated in Fig 7 for the ETC with $L = 1.5\lambda$. It can be seen that at both open $F_g = 4 \rightarrow F_e = 3, 4$ transitions, good-amplitude and SDW reduced-fluorescence dips occur with increasing light intensity. The situation differs from the completely closed $F_g = 4 \rightarrow F_e = 5$ transition – no dip occurs at the atomic transition centre.

Physical processes behind the narrow dip formations can be summarised as follows. For the open transitions, both two-level-system saturation and three-level-system optical pumping deplete the atomic population of the ground level excited by the light. The result of this velocity selective depleting (predominantly slow atoms accumulate on the ground level non-interacting with the laser light) is the narrow, reduced fluorescence dip centred at the open transition. As was proposed in Ref. [9], the situation is different from the completely closed $F_g = 4 \rightarrow F_e = 5$ transition. Here, the two-level-system saturation process decreases the ground level population, while the fluorescence decay back to this level increases its population in a narrow frequency interval, as the optical accumulation of atoms via fluorescence cycles is a relatively slow process. The total result is a small enhancement of the fluorescence signal in a narrow spectral region centred at the optical transition.

Very recently we have reported the first observation of a narrow, reduced fluorescence feature also in the profile of the completely closed $F_g = 4 \rightarrow F_e = 5$ transition at $L = (2-3)\lambda$ [13]. To illustrate the new structure, we present the ETC fluorescence spectra for the set of $F_g = 4$ transitions in a cell with $L = 1.5\lambda$ and 2λ (Fig. 8). It can be seen that for both ETC thicknesses, the two open $F_g = 4 \rightarrow F_e = 3, 4$ transitions show SDW reduced absorption dips at the centre frequency of each fluorescence profile. However, the profile of the closed $F_g = 4 \rightarrow F_e = 5$ transition show different shapes for the two different values of L, namely no dip in the fluorescence is observed at $L = 1.5\lambda$, while a very small one appears at $L = 2\lambda$. We attribute this difference to the fact that while at $L = 1.5\lambda$ the Dicke effect is well presented in the absorption (Fig. 6), at $L = 2\lambda$ it vanishes (see Ref. [9]).

Thus, the well pronounced Dicke peak in the absorption spectrum can be the reason for the dip absence in the fluorescence at $L = 1.5\lambda$, i.e. even being a incoherent process, the fluorescence keeps some traces of the absorption behaviour, based on the coherent Dicke narrowing. Note that in the ETC different velocity groups of atoms contribute to absorption and fluorescence.

In case of the closed transition and $L = 2\lambda$, the assumed physical processes behind the new dip formation are based on the degeneracy of the two-level system. As was shown in Ref. [10], if the $F_g = 4 \rightarrow F_e = 5$ transition is excited by linearly polarised light (as in our experiment), Cs atoms accumulate on the $F_g = 4$ Zeeman sublevels with the highest probability

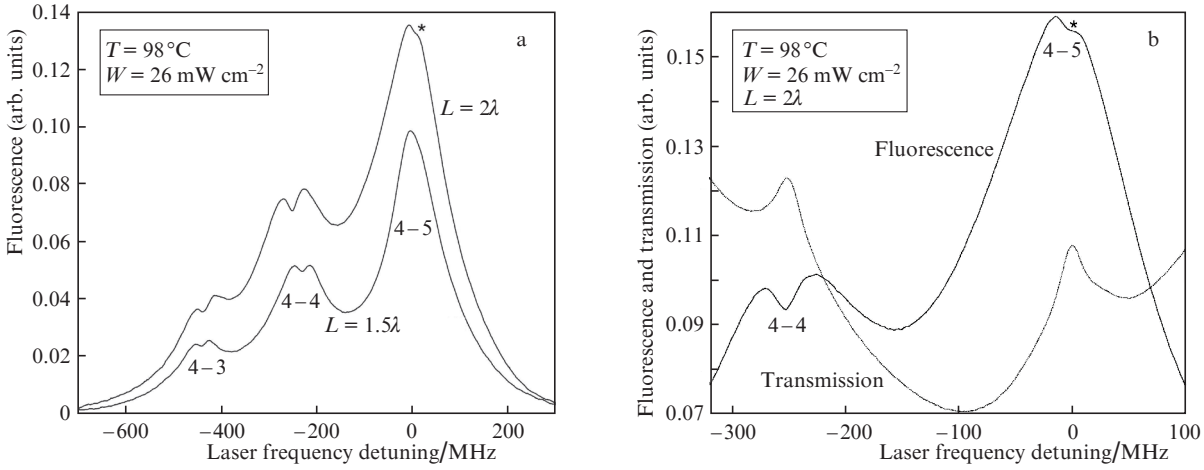

Figure 8. (a) Fluorescence spectra of the set of $F_g = 4$ transitions observed in the ETC of thickness $L = 1.5\lambda$ and 2λ at the atomic density $\sim 1.2 \times 10^{13}$ atom cm^{-3}. (b) Zoom of the spectrum showing the SDW feature in the fluorescence and transmission of the $F_g = 4 \rightarrow F_e = 5$ transition. The new dip in the fluorescence profile observed at $L = 2\lambda$ is marked by an asterisk.

of excitation, i.e. the highest fluorescence is expected for slow atoms [9]. However, in the case of depolarisation of the excited level, a significant portion of slow atoms will be accumulated on the $F_g = 4$ Zeeman sublevels with the lowest probability of excitation [10]. Hence, the excited state depolarisation will result in the efficiency loss during the excitation process of the atomic system even it does not suffer population loss. The reduction in the optical transition excitation rate will be the most significant for slow atoms, resulting in narrow dip formation in the fluorescence profile. The assumed depolarisation of the excited level can be caused by means of collisions between Cs atoms or by the influence of the cell window, as suggested in [11].

To avoid the influence of the Dicke coherent effect and to analyse the new dip in the fluorescence spectra under certain conditions, we present experimental results related to the absorption and fluorescence spectra for the set of $F_g = 4$ transitions at $L = 6\lambda$, where the Dicke effect influence vanishes completely. Moreover, while still avoiding CO resonances, a slight increase in the ETC thickness allows working at a lower atomic concentration, where the collisions between Cs atoms can be neglected. Figure 9 shows the fluorescence and transmission spectra obtained for $L = 6\lambda$ at significantly lower atomic source temperatures than that in Fig. 8. For the $F_g = 4 \rightarrow F_e = 5$ transition, a very well pronounced narrow pick ($\sim$15 MHz) in the absorption, as well as a sharp top of the fluorescence profile is observed. This interesting absorption peak is observed only at a very low atomic concentration and light intensity [9, 14], which is due to the fact that the $F_g = 4 \rightarrow F_e = 5$ transition is completely closed. In this case, the excited atoms can just turn back to their initial ground level due to spontaneous emission. However, during the spontaneous decay a velocity selective accumulation to the ground magnetic sublevels of slow atoms takes place, leading to the formation of a narrow peak in absorption [9].

The presence of this enhanced absorption/fluorescence structure shows that the excited state depolarisation does not take place [10] under the conditions of a very low light intensity and a low atomic source temperature. Keeping the temperature in the interval $T = 40-70\,^{\circ}C$, i.e. atomic concentration $1.5 \times 10^{11} - 1.8 \times 10^{12}$ atom cm^{-3}, our experimental study has shown that the rising of the laser intensity leads to transformation of the enhanced absorption/fluorescence resonance to a reduced absorption/fluorescence one – the higher the temperature the lower the light intensity for the resonance sign transformation. For instance, at $T = 60\,^{\circ}C$, the light intensity enhancement to 7 mW cm^{-2} results in the resonance sign reversal.

Figure 10 shows the absorption and fluorescence spectra obtained for $L = 6\lambda$ at two higher atomic source temperatures, namely $T = 87\,^{\circ}C$ (atomic density of 5.9×10^{12} atom cm^{-3}) and $T = 98\,^{\circ}C$. For the two open transitions, reduced absorption/fluorescence resonances are observed. Moreover, at the closed $F_g = 4 \rightarrow F_e = 5$ transition, the formation of the reduced absorption/fluorescence resonance is clearly seen even at the low light intensity. Note that the resonances formed at the closed transition are narrower than those at the open transitions.

Concerning the new reduced-fluorescence resonance formation, the assumed physical processes are related to the depolarisation of the excited level, which will transform the completely closed system to one with effective loss in the excitation process. It is difficult to separate the two main processes that can be responsible for the excited level magnetic sublevel population mixing, namely the elastic interaction between Cs atoms at enhanced atomic vapour pressures and the elastic interaction between the cell windows and the Cs atoms travelling parallel to the windows surface, which was proposed phenomenologically in the theoretical modelling performed in Ref. [11].

In the presented work, we discuss in more details the influence of the ETC windows on the excited state population mixing. This role is particularly important and most probably dominating when lower atomic source temperatures are used in the experiment (Fig. 9). Our estimates show that for $T = 60\,^{\circ}C$, the number of elastic collisions between Cs atoms is of low probability because the mean free path between two collisions (1.2 mm) is comparable with the laser beam diameter. However, the experimental results show that even for such a low temperature, the resonance sign reversal takes place with the light intensity rising to 7 mW cm^{-2}, which increases the population of the $F_e = 5$ level. At higher atomic source temperature (Fig. 10), the reduced fluorescence SDW resonance is observed even for a very low light intensity. At $T = 100\,^{\circ}C$

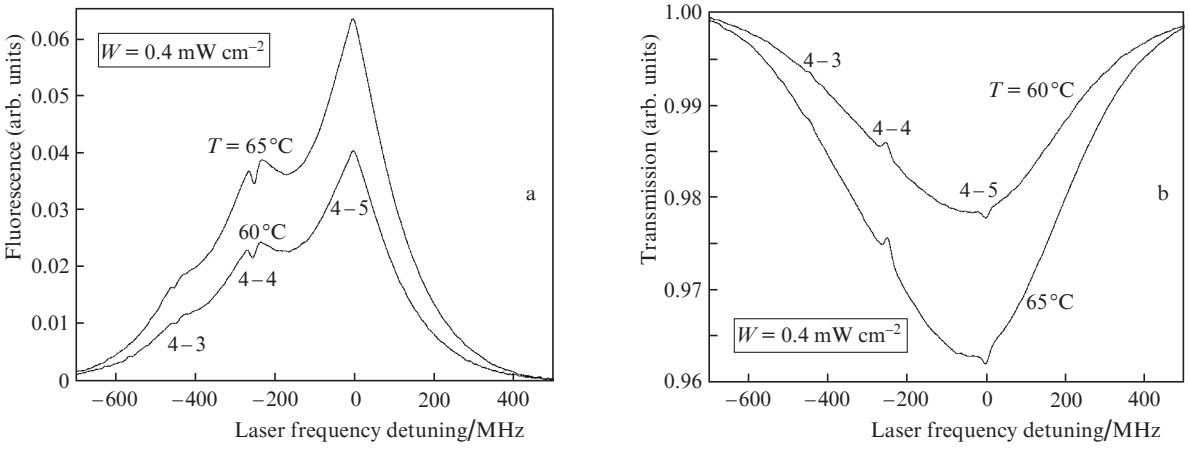

Figure 9. (a) Fluorescence and (b) transmission spectra of the set of $F_g = 4$ transitions observed in the ETC of thickness $L = 6\lambda$. The dips of reduced transmission (enhanced absorption) centred at the $F_g = 4 \rightarrow F_e = 5$ transition (b) are clearly seen for the case of low light intensity and lower atomic concentrations: $\sim 8.4 \times 10^{11}$ atom cm^{-3} ($T = 60\,^{\circ}C$) and $\sim 1.2 \times 10^{12}$ atom cm^{-3} ($T = 65\,^{\circ}$).

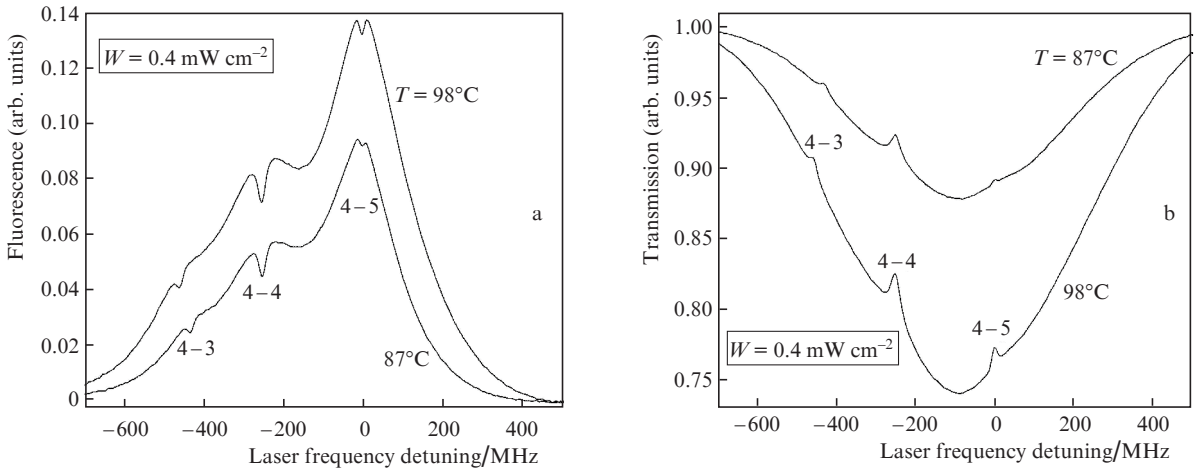

Figure 10. (a) Fluorescence and (b) transmission spectra of the set of $F_g = 4$ transitions observed in the ETC of thickness $L = 6\lambda$. For a higher atomic concentration a narrow dip in the fluorescence occurs at the closed $F_g = 4 \rightarrow F_e = 5$ transition.

the time interval estimated between two Cs–Cs collisions (~360 ns) is still an order of magnitude larger than the lifetime of the excited state (about 30 ns). Thus, the mixing of the excited state Zeeman sublevel population due to Cs–Cs collisions is also of low probability, which can be considered in support of the ETC window surface influence on the excited atomic state polarisation.

When atoms are moving in the ETC, they can undergo both elastic and inelastic collisions with the cell windows. In this way the spectroscopy of the ETC provides the possibility to study the atom–surface interactions. If the atom flies very close to the surface, it can 'feel' the periodic potential of the crystal surface of the thin cell. The effect concerning the atom–surface interaction has been known as the long-range van der Waals (vdW) attraction between the atom (in ground or excited state) and the dielectric surface (YAG windows) when the distance is ~100 nm. This effect may cause a shift or broadening of the atomic transition, both in transmission and fluorescence [15]. So far the influence of the long-range vdW force on the polarisation of the excited state has not been investigated. In our work we consider such an influence on polarisation as probable in analogy with the behaviour of the bright CPT resonance in a conventional buffered cell containing Cs atoms. It has been shown [10] that the bright CPT resonance observed in evacuated conventional cells transforms into a dark resonance when a buffer gas is added. The resonance sign reversal there is attributed to depolarisation of the excited state by the elastic collisions between alkali and noble gas atoms. It is well known that the last type of collisions causes also a shift and broadening of atomic transitions.

3. Theoretical modelling and discussions

We use the theoretical model [8] based on solving the optical Bloch equations for a two-level system. In order to analyse the behaviour of the $F_g = 3$ transitions, the simulations are performed for the open hyperfine transitions. As an open system we consider one with losses by a spontaneous emission to a generic 'third level'. Levels 1 and 2 are coupled by a laser light at a frequency ω detuned by Δ from the transition frequency ω_{21} ($\Delta = \omega - \omega_{21}$). The parameters used are chosen to be applicable to a realistic alkali system namely: $\gamma_{21} = 5$ MHz, $ku = 250$ MHz and $\alpha = 0.6$ (γ_{21} is half the transition rate of the exited state, ku is the most probable Doppler shift of the emitted light and α is the probability to decay from level 2 to level 1). The system of Bloch equations has the form

$$v\frac{d\sigma_{21}}{dz} + D_{21}\sigma_{21} - i\frac{\Omega_R}{2}(\sigma_{11} - \sigma_{22}) = 0, \quad (1)$$

$$v\frac{d\sigma_{22}}{dz} + \gamma_2\sigma_{22} - \Omega_R \operatorname{Im}\sigma_{21} = 0, \quad (2)$$

$$v\frac{d\sigma_{11}}{dz} - \alpha\gamma_2\sigma_{22} + \Omega_R \operatorname{Im}\sigma_{21} = 0, \quad (3)$$

where Ω_R is the Rabi frequency of the transition; $D_{21} = \gamma_{21} + ikv - i\Delta$; v is the atomic velocity; and σ_{ij} are the reduced density matrix elements in the rotating frame.

The absorption is given by

$$A = \int_0^\infty G(v)\exp\left[-\left(\frac{kv}{ku}\right)^2\right]dv, \quad (4)$$

where

$$G(v) = \int_0^L \operatorname{Im}[\sigma_{21}(z,v)]\,dz.$$

The fluorescence is proportional to U

$$U = \int_0^\infty Q(v)\exp\left[-\left(\frac{kv}{ku}\right)^2\right]dv, \quad (5)$$

where

$$Q(v) = \int_0^L [\sigma_{22}(z,v)]\,dz.$$

First we present the results of simulations for the open transitions within the D_2 line. Figure 11 shows the fluorescence profiles for the open transition at the ETC thickness from $L = \lambda$ up to 6λ. Due to the population loss introduced by hyperfine/Zeeman optical pumping, well pronounced narrow dips are observed at the centre of the optical transition for all examined cell thicknesses. It can be seen that the amplitude and the contrast of the dips grow fast with the cell thickness. Hence, the performed theoretical simulations allowed us to predict strong enhancement of the fluorescence dip contrast

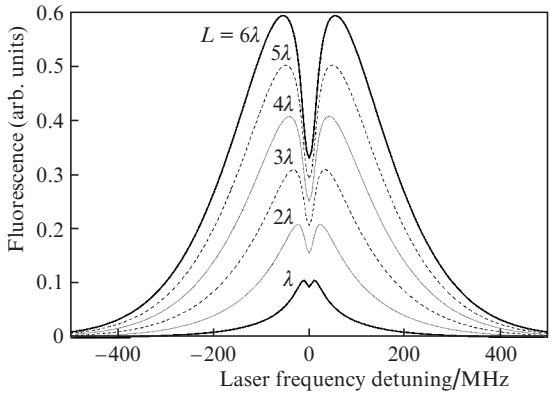

Figure 11. Theoretical calculations of the fluorescence profiles for open transition at different L. The light intensity is $W = 20$ mW cm^{-2}.

with the cell thickness, thus stimulating the systematic experimental study performed for the ETC with $L = 6\lambda$.

We should keep in mind that the fluorescence dip comes mainly from very slow atoms, whose velocity component on the laser beam propagation direction is small enough to allow the needed time for several cycles of absorption of photons with subsequent spontaneous emissions. For this reason it is advantageous to use low atomic concentrations (low ETC atomic source temperature) in order to avoid collisions between Cs atoms. It is interesting to determine to what extent the lower atomic density can be compensated by the laser light intensity enhancement.

Theoretical profiles were calculated for different intensities, showing slow reduced fluorescence dip broadening with increasing light intensity. From the theoretical profiles, two important parameters were determined: contrast and FWHM of the reduced fluorescence dip formed at the optical transition centre. The theoretically obtained SDW resonance contrast and width are compared with the experimentally measured corresponding parameters from the experimental spectra similar to those shown in Fig. 5. The obtained result is shown in Fig. 12. It can be seen that the simple two-level theoretical model, which involves relaxation to a third level by spontaneous decay, very well describes the dip width and contrast behaviour with the light intensity.

The fluorescence dip broadening with increasing light intensity is attributed to the enhanced optical pumping rate [16] that leads to enlargement of the velocity interval for atoms involved in the optical pumping process. The dip contrast improvement with increasing light intensity is also due to the increased rate of optical pumping, which results in a higher value velocity selective atomic population loss from the $F_g = 3$ level [17]. The results presented in Fig.12 support the potential of the ETC with $L = 6\lambda$ for development of frequency reference due to the very good contrast-to-width ratio, which mainly determines the merit of the frequency reference. This ratio is almost constant within the used light intensity interval.

The second simulation is related to the analysis of the saturation of transmission profile, in the presence of Dicke effect. In case of the first Dicke revival ($L = 1.5\lambda$), the theoretical simulation of the transmission profile concerning the closed atomic transition is performed for two important cases – low and high light intensities (Fig. 13). At a low light intensity (0.2 mW cm^{-2}), the calculated transmission profile of the closed transition shows a narrow Dicke structure, which is

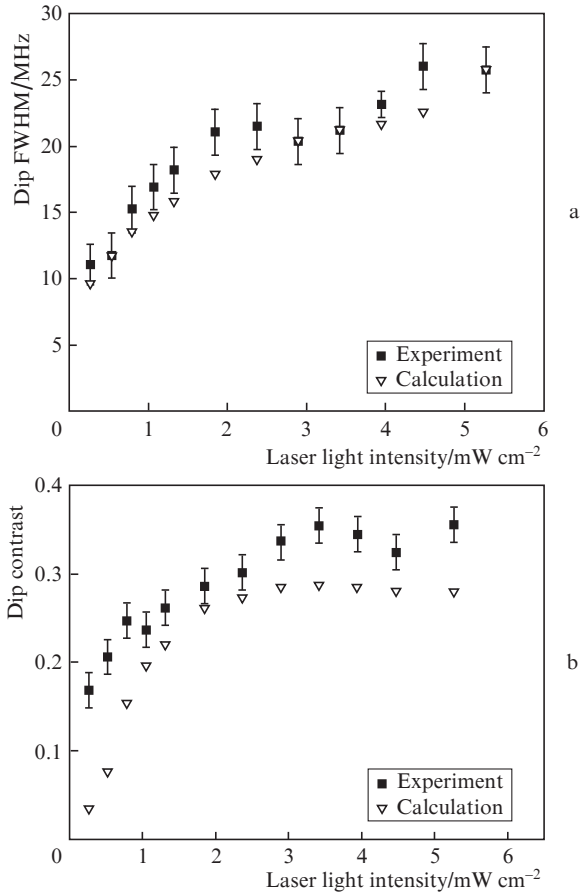

Figure 12. (a) Experimental and theoretical fluorescence dip FWHM and (b) dip contrast vs. light intensity. Experimental curves are obtained for the $F_g = 3 \rightarrow F_e = 2$ transition, the atomic source temperature is $T = 68$ °C.

superimposed on a broad pedestal. Comparing the experimental results presented in Fig. 6 with the theoretical profile shown in Fig. 13, the good agreement can be pointed out. At a higher light intensity (20 mW cm^{-2}), the simulation shows that together with the absorption dip the closed transition profile exhibits also a narrow absorption peak superimposed on the broader dip. The two features are well pronounced both in the experiment (Fig. 6) and the theory (Fig. 13), in the case of saturated regime.

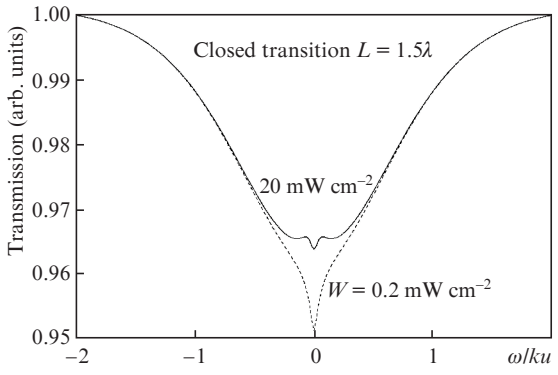

Figure 13. Theoretical simulation of the saturation behaviour of the closed transition in case of the first Dicke revival.

To analyse the new dip, observed experimentally in the fluorescence profile of the closed $F_g = 4 \rightarrow F_e = 5$ transition, an extremely small loss was introduced in the system of the completely closed two-level transition, namely the value of $\alpha = 0.99$ was taken. The assumed physical processes behind such a loss are based on the degeneracy of the two-level system. As discussed in Section 2, if the $F_g = 4 \rightarrow F_e = 5$ transition is excited by linearly polarised light, Cs atoms accumulate on the $F_g = 4$ Zeeman sublevels with the highest probability of excitation, i.e. the highest fluorescence is expected for slow atoms emitting in a narrow spectral interval around the centre frequency of the atomic transition [9]. However, in the case of depolarisation of the excited level, a significant portion of slow atoms will be accumulated on the $F_g = 4$ Zeeman sublevels with the lowest probability of excitation [10]. Hence, the excited state depolarisation will transform the system with no population loss to the third level to one suffering reduced rate of excitation.

The simulated fluorescence profiles of the $F_g = 4 \rightarrow F_e = 5$ transition for $\alpha = 0.99$, which means a slightly open two-level system, are presented in Fig. 14 for the ETC with $L = \lambda$, 1.5λ, 2λ, 2.5λ and 3λ. It can be seen that already at $L \geqslant 2\lambda$ even extremely small opening of the two-level system results in observation of the saturation dip centred at the optical transition. As in the experimental observations, the amplitude of the dip increases with increasing ETC thickness.

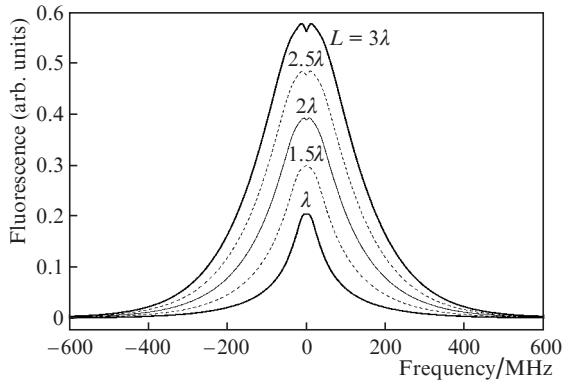

Figure 14. Theoretical fluorescence spectra calculated at $\alpha = 0.99$, different thicknesses L and laser intensity 35 mW cm^{-2}.

To estimate the influence of the excited level depolarisation on the atomic excitation process, following the rate equation model developed in Ref. [18], we first calculated the atomic population density on each magnetic sublevel of the ground and excited levels of the $F_g = 4 \rightarrow F_e = 5$ transition, with no depolarisation of the $F_e = 5$ level. The rate equation system describes the evolution of the population of magnetic sublevels as a result of the spontaneous/stimulated transitions between the ground and excited magnetic sublevels. Linear polarisation of the laser beam is considered. The summary population of the $F_e = 5$ level is determined.

After that the rate equation system was modified in order to involve the mixing of the excited magnetic sublevel populations, caused by the elastic interactions between Cs atoms and the Cs atoms with the windows of the ETC. Different rates of population mixing between magnetic sublevels of the $F_e = 5$ level were taken into account, and for each one the net population of the $F_e = 5$ level was determined. The obtained results are presented in Fig. 15. It can be seen that the population of the $F_e = 5$ level is reduced significantly by its depolarisation. It can be estimated from Fig. 15 that the introduction of atomic population mixing at a low rate ($r = 0.055$) results in 1.4% drop of the population of the $F_e = 5$ level when compared with the case where there is no depolarisation ($r = 0$). Hence, a small number of depolarising collisions can cause a measurable reduction in the $F_e = 5$ level population.

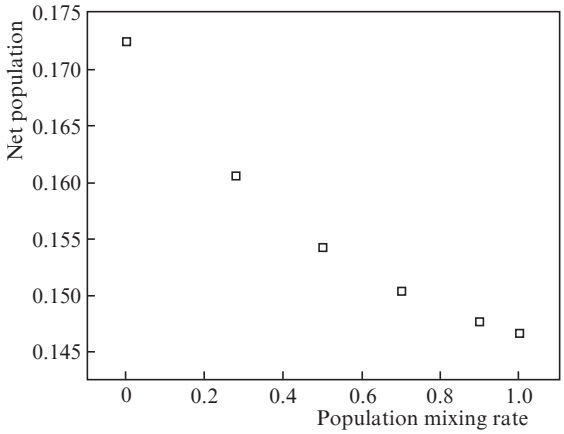

Figure 15. Net population of the $F_e = 5$ level as a function of the population mixing rate among Zeeman sublevels.

Going back to Fig.14, which shows that small loss in the slightly open two-level system results in a well-pronounced dip in the fluorescence profile, one can conclude that the closed $F_g = 4 \rightarrow F_e = 5$ transition on the D_2 line of Cs atoms confined in the ETC can find application in the investigations of atom–atom and atom–dielectric surface elastic collisions.

4. Conclusions

The miniaturisation of practical devices based on alkali atomic vapour confined in optical cells is of rising interest for the development of photonic sensors. In this paper we discuss how the optical cell thickness miniaturisation process affects the parameters of the SDW resonance observed in Cs-filled vacuum cells.

The theoretical simulation of the fluorescence profiles of open hyperfine transitions in the ETC of different cell thicknesses shows that the contrast of the SDW features observed in the optical transition profiles increases with increasing ETC thickness. This prediction is confirmed experimentally by the observation of a narrow reduced fluorescence dip in the hyperfine transition fluorescence profile, which is with an order of magnitude higher contrast for the ETC with $L = 6\lambda$ than that with $L = \lambda$. Thus, a small increase in the ETC thickness makes it advantageous to use the narrow dips in the fluorescence profiles as frequency references for laser frequency stabilisation. An additional advantage of the ETC thickness enhancement is related to the reduction of light intensity and atomic source temperature needed for the narrow resonance formation.

A theoretical simulation is performed to analyse the physical processes behind the SDW resonance sign reversal for closed atomic transitions. The model involves elastic interactions between Cs atoms as well as elastic interaction between atoms and ETC windows, both resulting in depolarisation of

the excited state, which can lead to the observations of new effects.

It is important to note that the presented narrow optical resonances formed in Cs vapours have been successfully implemented in the case of Rb vapour (also contained in the ETC) to study quantitatively individual atomic transition behaviour in a very strong magnetic field up to 0.5 T. Also, possible applications were described, such as magnetometers with nanometric local spatial resolution and tunable atomic frequency references [19, 20].

Acknowledgements. The work was partially supported by the Marie Curie International Research Staff Exchange Scheme Fellowship (Grant Agreement No. PIRSES-GA-295264) and Indian-Bulgarian (BIn-2/07) bilateral contract.

References

1. Sarkisyan D., Bloch D., Papoyan A., Ducloy M. *Opt. Commun*., **200**, 201 (2001).
2. Romer R.H., Dicke R.H. *Phys. Rev*., **99**, 532 (1955).
3. Dutier G., Saltiel S., Bloch D., Ducloy M. *J. Opt. Soc. Am. B*, **20**, 793 (2003).
4. Sarkisyan D., Varzhapetyan T., Sarkisyan A., Malakyan Yu., Papoyan A., Lezama A., Bloch D., Ducloy M. *Phys. Rev. A*, **69**, 065802 (2004).
5. Dutier G., Yarovitski A., Saltiel S., Papoyan A., Sarkisyan D., Bloch D., Ducloy M. *Europhys. Lett*., **63**, 35 (2003).
6. Briaudeau S., Saltiel S., Nihenius G., Bloch D., Ducloy M. *Phys. Rev. A*, **57**, R3169-R3172 (1998).
7. Vartanyan T.A., Lin D.L. *Phys. Rev. A*, **51**, 1959 (1995).
8. Andreeva C., Cartaleva S., Petrov L., Saltiel S.M., Sarkisyan D., Varzhapetyan T., Bloch D., Ducloy M. *Phys. Rev. A*, **76**, 013837 (2007).
9. Cartaleva S., Saltiel S., Sargsyan A., Sarkisyan D., Slavov D., Todorov P., Vaseva K. *J. Opt. Soc. Am. B*, **26**, 1999 (2009).
10. Andreeva C., Cartaleva S., Dancheva Y., Biancalana V., Burchianti A., Marinelli C., Mariotti E., Moi L., Nasyrov K. *Phys. Rev. A*, **66**, 012502 (2002).
11. Andreeva C., Atvars A., Auzinsh M., Bluss K., Cartaleva S., Petrov L., Slavov D. *Phys. Rev. A*, **76**, 063804 (2007).
12. Schmidt O., Knaak K.M., Wynands R., Meschede D. *Appl. Phys. B*, **59**, 167 (1994).
13. Cartaleva S., Sargsyan A., Sarkisyan D., Slavov D., Vaseva K. *Proc. SPIE Int. Soc. Opt. Eng*., **7747**, 77470H (2011).
14. Biancalana V., Cartaleva S., Dancheva Y., Gosh P.N., Mariotti E., Mitra S., Moi L., Petrov N., Ray B., Sarkisyan D., Slavov D. *Acta Polonica A*, **116**, 495 (2009).
15. Hamdi I., Todorov P., Yarovitski A., Dutier G., Maurin I., Saltiel S., Li Y., Lezama A., Varzhapetyan T., Sarkisyan D., Gorza M.-P., Fichet M., Bloch D., Ducloy M. *Laser Phys*., **15**, 987 (2005).
16. Sargsyan A., Sarkisyan D., Papoyan A., Pashayan-Leroy Y., Moroshkin P., Weis A., Khanbekyan A., Mariotti E., Moi L. *Laser Phys*., **18**, 749 (2008).
17. Briaudeau S., Bloch D., Ducloy M. *Europhys. Lett*., **35**, 337 (1996).
18. Krasteva A., Slavov D., Cartaleva S. *Intern. J. Opt*., Article ID 683415 (2011).
19. Sargsyan A., Hakhumyan G., Papoyan A., Sarkisyan D., Atvars A., Auzinsh M. *Appl. Phys. Lett*., **93**, 021119 (2008).
20. Hakhumyan G., Leroy C., Pashayan-Leroy Y., Sarkisyan D., Auzinsh M. *Opt. Commun*., **284**, 4007 (2011).